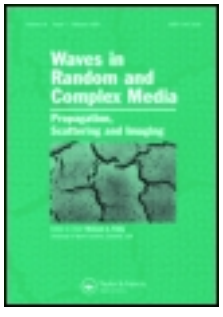

Waves in Random and Complex Media
Publication details, including instructions for authors and subscription information:
http://www.tandfonline.com/loi/twrm20

Two-dimensional radiative transfer due to curved Dirac delta line sources

André Liemert[a] & Alwin Kienle[a]
[a] Institut für Lasertechnologien in der Medizin und Meßtechnik, Ulm, Germany.
Published online: 04 Nov 2013.

To cite this article: André Liemert & Alwin Kienle , Waves in Random and Complex Media (2013): Two-dimensional radiative transfer due to curved Dirac delta line sources, Waves in Random and Complex Media, DOI: 10.1080/17455030.2013.851430

To link to this article: http://dx.doi.org/10.1080/17455030.2013.851430

Waves in Random and Complex Media, 2013
http://dx.doi.org/10.1080/17455030.2013.851430

Taylor & Francis
Taylor & Francis Group

Two-dimensional radiative transfer due to curved Dirac delta line sources

André Liemert* and Alwin Kienle

Institut für Lasertechnologien in der Medizin und Meßtechnik, Ulm, Germany

(*Received 31 May 2013; accepted 29 September 2013*)

In this article, the two-dimensional radiative transport equation is considered for the curved Dirac delta line source. In order to account this source type, Green's function of the radiative transport equation for the half-plane is derived in parts of the ballistic and diffuse contribution as well as under consideration of the Fresnel reflection at the boundary. The final results are verified with the Monte Carlo method for different collimated beams and several curved sources such as the elliptic and logarithmic spiral line source.

Introduction

The radiative transport equation (RTE) is the fundamental equation for describing the propagation of waves and particles in random media. Important examples are the transport of neutrons in reactor physics, the propagation of photons in material science, in astronomy, or in biophotonics.[1–4] In recent time, the RTE has been solved for infinitely extended and bounded media under consideration of commonly used source types such as directed beams, isotropic point sources, and infinitely long straight line sources.[5–9] The more general case of curved Dirac delta line sources has not been described analytically so far. In general, the Dirac delta line function is often encountered in electromagnetic and biological problems when a long and thin structure is involved. For example, a distribution of electric charge along a curve or flexible structures such as elastic fibers can be treated as a smooth curve.[10,11] Further applications in the acoustics field can be found in [12].

In this article, we describe the Dirac delta line function embedded in a plane where the elliptic line is discussed in detail. In order to apply the line source formalism in radiative transfer calculations, we afore provide an analytical half-space Green's function for the anisotropically scattering plane, the so-called *flatland* geometry. The flatland is in principle a three-dimensional (3D) world where all objects are infinitely extended along one direction. The corresponding physical phase space of the flatland is characterized by two spatial and one angular variables. The derived Green's function itself can be applied for real two-dimensional (2D) problems, e.g. for studying the light propagation in thin films,[13] for modeling the propagation of waves in surfaces with random impedances,[14] or for describing wave scattering in the marginal ice zone.[15] In cases when the light beam is incident perpendicularly to the axes of optically infinitely extended fibers, the scattered photons remain in a plane, the flatland, so that the 2D RTE realistically models the transport

*Corresponding author. Email: andre.liemert@ilm.uni-ulm.de

process. An important example for this scenario is given by the carbon fiber-reinforced materials. A formal derivation of the flatland RTE inclusive some further theoretical aspects can be found in [16,17]. The corresponding diffusion equation with appropriate boundary conditions (BC) is presented in [18].

In our recent study,[19] we already considered the 2D RTE where the effect of the Fresnel reflection has not been taken into account and the final solutions are based on inhomogeneous BC. The use of boundary sources however leads to numerical instabilities which results in considerable limitations regarding the evaluation of the obtained equations. Moreover, the case of an isotropic point source within a semi-infinite half-plane has also not been discussed before. Therefore, our recent work is both extended and revised in view of the numerical stability and the treatment of the BC. Besides direct applications of the derived equations, a further important aspect is that it can be used for verification of other RTE solvers such as the Monte Carlo method or the finite-volume method.[20,21] The solution to the boundary-value problem in the bounded flatland geometry is successfully verified with the Monte Carlo method.

Theory

Green's function of the 2D RTE

The specific intensity or radiance $G(\boldsymbol{\rho}, \phi)$ in the plane $z = 0$ caused by an unidirectional light beam which radiates in direction $\hat{\mathbf{s}}_0 = (\cos\phi_0, \sin\phi_0)$ obeys the 2D RTE

$$\cos\phi\frac{\partial G(\boldsymbol{\rho},\phi)}{\partial x}+\sin\phi\frac{\partial G(\boldsymbol{\rho},\phi)}{\partial y}+\mu_t G(\boldsymbol{\rho},\phi)=\mu_s\int_{\mathbb{S}^1} G(\boldsymbol{\rho},\phi')f(\hat{\mathbf{s}}\cdot\hat{\mathbf{s}}')\mathrm{d}\phi'+\delta(\boldsymbol{\rho})\delta(\phi-\phi_0), \tag{1}$$

where $\mu_t = \mu_a+\mu_s$ is the total attenuation coefficient, μ_a the absorption coefficient, μ_s the scattering coefficient, and ϕ_0 is the azimuthal angle of the light beam relative to the x-axis. The unit vector $\hat{\mathbf{s}} = (\cos\phi, \sin\phi)$ specifies the direction of the particle propagation and $f(\hat{\mathbf{s}}\cdot\hat{\mathbf{s}}')$ is the scattering phase function describing the direction of the scattered particles.

In the following Green's function is separated into its ballistic and diffuse contribution according to $G(\boldsymbol{\rho}, \phi) = G_b(\boldsymbol{\rho}, \phi) + I(\boldsymbol{\rho}, \phi)$. Substituting this ansatz in (1) leads to the first RTE

$$\cos\phi\frac{\partial G_b(\boldsymbol{\rho},\phi)}{\partial x}+\sin\phi\frac{\partial G_b(\boldsymbol{\rho},\phi)}{\partial y}+\mu_t G_b(\boldsymbol{\rho},\phi)=\delta(\boldsymbol{\rho})\delta(\phi-\phi_0), \tag{2}$$

whose solution gives the ballistic component

$$G_b(\boldsymbol{\rho},\phi)=\frac{e^{-\mu_t\rho}}{\rho}\delta(\phi_{\boldsymbol{\rho}}-\phi_0)\delta(\phi-\phi_0). \tag{3}$$

Taking into account this component, the second RTE for the diffuse part is obtained as

$$\begin{aligned}&\cos\phi\frac{\partial I(\boldsymbol{\rho},\phi)}{\partial x}+\sin\phi\frac{\partial I(\boldsymbol{\rho},\phi)}{\partial y}+\mu_t I(\boldsymbol{\rho},\phi)\\&=\mu_s\int_{\mathbb{S}^1} I(\boldsymbol{\rho},\phi')f(\hat{\mathbf{s}}\cdot\hat{\mathbf{s}}')\mathrm{d}\phi'+\mu_s\frac{e^{-\mu_t\rho}}{\rho}\delta(\phi_{\boldsymbol{\rho}}-\phi_0)f(\hat{\mathbf{s}}\cdot\hat{\mathbf{s}}_0),\end{aligned} \tag{4}$$

which must be solved subject to the BC defined in the angular domain $\hat{\mathbf{s}}\cdot\hat{\mathbf{x}} > 0$

$$I(x=0,y,\phi)=R(\phi)I(x=0,y,\pi-\phi). \tag{5}$$

Here $R(\phi) = R(-\phi)$ is the Fresnel reflection coefficient which is given by

$$R(\phi) = \frac{1}{2}\left(\frac{\sin^2(\phi-\phi')}{\sin^2(\phi+\phi')} + \frac{\tan^2(\phi-\phi')}{\tan^2(\phi+\phi')}\right), \quad |\phi| < \phi_c \tag{6}$$

and $R(\phi) = 1$ when $|\phi| > \phi_c$. Moreover $\phi_c = \arcsin(1/n)$ is the value for the critical angle of total reflection, $\phi' = \arcsin(n \sin\phi)$ is the angle of refraction given by Snell's law, and n denotes the relative refractive index. If $n < 1$ the critical angle becomes $\phi_c = \pi/2$. The RTE (4) can be translated into a system of coupled partial differential equations by expanding all angular-dependent quantities according to

$$I(\boldsymbol{\rho}, \phi) = \sum_{m=-N}^{N} \psi_m(\boldsymbol{\rho}) e^{im\phi}, \tag{7}$$

with $\psi_m(\boldsymbol{\rho}) = 0 \;\forall\; |m| > N$ and N is the expansion order. The rotationally invariant scattering phase function is given by the Fourier series

$$f(\hat{\mathbf{s}}\cdot\hat{\mathbf{s}}') = \frac{1}{2\pi}\sum_{m=-N}^{N} f_{|m|} e^{im(\phi-\phi')} = \frac{1}{2\pi} + \frac{1}{\pi}\sum_{m=1}^{N} f_m \cos[m(\phi-\phi')], \tag{8}$$

where the expansion coefficients are defined as

$$f_m = \int_0^{2\pi} f(\cos\theta)\cos(m\theta)\mathrm{d}\theta. \tag{9}$$

The specific intensity is a real quantity and hence the spatial-dependent moments satisfy the condition $\psi_m(\boldsymbol{\rho}) = \psi^*_{-m}(\boldsymbol{\rho})$. Inserting (7) in (4) leads to the following $2N+1$ coupled equations

$$\begin{aligned}&\left(\frac{\partial}{\partial x} - i\frac{\partial}{\partial y}\right)\psi_{m-1}(\boldsymbol{\rho}) + \left(\frac{\partial}{\partial x} + i\frac{\partial}{\partial y}\right)\psi_{m+1}(\boldsymbol{\rho}) + 2\sigma_m\psi_m(\boldsymbol{\rho})\\ &\quad = \mu_s \frac{e^{-\mu_t\rho}}{\pi\rho}\delta(\phi_{\boldsymbol{\rho}} - \phi_0) f_{|m|} e^{-im\phi_0},\end{aligned} \tag{10}$$

where $\sigma_m = \mu_a + (1 - f_{|m|})\mu_s$. By performing the one-dimensional Fourier transform

$$\psi_m(\boldsymbol{\rho}) = \frac{1}{2\pi}\int_{-\infty}^{\infty} \psi_m(x,k) e^{iky}\mathrm{d}k \tag{11}$$

we obtain a system of ordinary differential equations for $\psi_m = \psi_m(x,k)$

$$\frac{\mathrm{d}\psi_{m-1}}{\mathrm{d}x} + \frac{\mathrm{d}\psi_{m+1}}{\mathrm{d}x} + k(\psi_{m-1} - \psi_{m+1}) + 2\sigma_m\psi_m = \frac{\mu_s}{\pi}\frac{e^{-\Omega_0 x}}{\cos\phi_0}\Theta(x) f_{|m|} e^{-im\phi_0}, \tag{12}$$

where $\Omega_0 = \mu_t/\cos\phi_0 + ik\tan\phi_0$ and $\Theta(x)$ is the Heaviside step function. The symmetry condition in Fourier space is $\psi_m(x,k) = \psi^*_{-m}(x,-k)$. The particular solution of the above system can be evaluated efficiently by seeking a similar solution in the scattering domain $x > 0$ according to $\psi_m^{(p)}(x,k) = e^{-\Omega_0 x} I_m(k)$. Therefore, we obtain

$$(k-\Omega_0) I_{m-1}(k) - (k+\Omega_0) I_{m+1}(k) + 2\sigma_m I_m(k) = \frac{\mu_s}{\pi} f_{|m|}\frac{e^{-im\phi_0}}{\cos\phi_0}. \tag{13}$$

The general solution to the homogenous problem which vanish for $x \to \infty$ has the form $\psi_m^{(h)}(x,k) = e^{-\xi x}\psi_m(k)$. In order to avoid a numerical solution of a k-dependent eigenvalue problem (EVP), we perform the product ansatz $\psi_m(k) = a_m\varphi_m$. Inserting this ansatz in (12) and setting the right-hand side equal to zero leads to

$$-(\xi - k)a_{m-1}\varphi_{m-1} - (\xi + k)a_{m+1}\varphi_{m+1} + 2\sigma_m a_m\varphi_m = 0. \tag{14}$$

A further condition is needed so that we can require $(\xi - k)a_{m-1} = (\xi + k)a_{m+1}$. One solution of this difference equation is given by $a_m = [(\xi - k)/(\xi + k)]^{m/2}$. Taking into account this solution leads to the following simplified EVP for $|m| \leq N$ with $\varphi_{|m|>N} = 0$

$$\sqrt{\xi^2 - k^2}\varphi_{m-1} + \sqrt{\xi^2 - k^2}\varphi_{m+1} - 2\sigma_m\varphi_m = 0. \tag{15}$$

In matrix notation we can write $(\nu A - S^2)\,|\varphi\rangle = 0$, where S is a diagonal matrix with elements $S_{mm'} = \sqrt{2\sigma_m}\delta_{mm'}$ and $\nu = \sqrt{\xi^2 - k^2}$. By applying the inverse S^{-1} having the diagonal elements $S^{-1}_{mm'} = \delta_{mm'}/\sqrt{2\sigma_m}$, the EVP becomes $\left(S^{-1}AS^{-1}\right)S\,|\varphi\rangle = S\,|\varphi\rangle\,/\nu$. Thus, if λ is an eigenvalue of $S^{-1}AS^{-1}$ corresponding with the eigenvector $|u\rangle$, one obtains $\nu = 1/\lambda$ and hence $\xi = \sqrt{k^2 + 1/\lambda^2}$. The corresponding eigenvectors are given by $|\varphi\rangle = S^{-1}\,|u\rangle$ so that the k-independent solution of (15) becomes $\varphi_m = u_m/\sqrt{2\sigma_m}$. The matrix $S^{-1}AS^{-1}$ is symmetric and tridiagonal having $2N + 1$ real-valued eigenvalues $0, \pm\lambda_1, \pm\lambda_2, \ldots, \pm\lambda_N$. Note that the eigenvectors $|u\rangle$ are assumed to be normalized to unity which is required later. The complete homogenous solution is now given via superposition

$$\psi_m^{(h)}(x,k) = \sum_{i=1}^{N} C_i(k)\varphi_m^{(i)} e^{-\sqrt{k^2+1/\lambda_i^2}\,x}\left[\sqrt{1 + (k\lambda_i)^2} - k\lambda_i\right]^m, \tag{16}$$

where $C_i(k) = C_i^*(-k)$ are the N unknown constants which are determined by using the BC, see below. Here the homogeneous solution is completed by the N positive eigenvalues $\lambda_i > 0$ because $\lambda_0 = 0$ is impossible and $\lambda_i < 0$ leads to the same eigenfunctions as the positive values. The resulting moments in Fourier space become $\psi_m(x,k) = \psi_m^{(h)}(x,k) + \psi_m^{(p)}(x,k)$. The unknown constants within the homogenous solution (16) in Fourier space are determined by setting Marshak-type conditions [22]

$$\int\limits_{\hat{\mathbf{s}}\cdot\hat{\mathbf{x}}>0} I(0,k,\phi)e^{-in\phi}\mathrm{d}\phi = \int\limits_{\hat{\mathbf{s}}\cdot\hat{\mathbf{x}}>0} R(\phi)I(0,k,\pi-\phi)e^{-in\phi}\mathrm{d}\phi, \tag{17}$$

so that we can create a system of N linear equation for $|n| = 0, 2, \ldots, N-1$ in order to find N unknown constants. By inserting the Fourier series in (17) and integrating both sides over the semicircle $\hat{\mathbf{s}}\cdot\hat{\mathbf{x}} > 0$, one can write

$$\sum_{m=-N}^{N}\psi_m(0,k)\,\mathrm{sinc}\left(\frac{m-n}{2}\right) = \frac{1}{\pi}\sum_{m=-N}^{N}(-1)^m\psi_m(0,k)\int\limits_{\hat{\mathbf{s}}\cdot\hat{\mathbf{x}}>0} R(\phi)\cos[(m+n)\phi]\mathrm{d}\phi, \tag{18}$$

where $\mathrm{sinc}(x) = \sin(\pi x)/(\pi x)$. Taking into account the symmetry relations above we obtain the spatial-dependent moments for the specific intensity (7) as

$$\psi_m(\boldsymbol{\rho}) = \frac{1}{2\pi}\int_0^\infty \psi_m(x,k)e^{iky} + \psi_{-m}^*(x,k)e^{-iky}\mathrm{d}k. \tag{19}$$

At this stage the solution becomes complete by adding the ballistic contribution (3).

In many applications, the reflectance and the internal fluence are quantities of particular interest. By making use of the derived specific intensity, we find for the current

$$\mathbf{J}(\boldsymbol{\rho}) = \int_{2\pi} \hat{\mathbf{s}} G(\boldsymbol{\rho}, \phi) \mathrm{d}\phi = \frac{e^{-\mu_t \rho}}{\rho} \delta(\phi_{\boldsymbol{\rho}} - \phi_0) \begin{pmatrix} \cos\phi_0 \\ \sin\phi_0 \end{pmatrix} + \begin{pmatrix} J_x(\boldsymbol{\rho}) \\ J_y(\boldsymbol{\rho}) \end{pmatrix}, \tag{20}$$

where $J_x(\boldsymbol{\rho}) = 2\pi\,\mathrm{Re}[\psi_1(\boldsymbol{\rho})]$ and $J_y(\boldsymbol{\rho}) = -2\pi\,\mathrm{Im}[\psi_1(\boldsymbol{\rho})]$. The reflected light at the boundary $x = 0$ of the scattering half-plane is given by the emergent current component $R(y) = \mathbf{J}(0, y) \cdot (-\hat{\mathbf{x}}) = -J_x(0, y)$, whereas the internal fluence becomes

$$\Phi(\boldsymbol{\rho}) = \int_{2\pi} G(\boldsymbol{\rho}, \phi) \mathrm{d}\phi = \frac{e^{-\mu_t \rho}}{\rho} \delta(\phi_{\boldsymbol{\rho}} - \phi_0) + 2\pi\,\psi_0(\boldsymbol{\rho}). \tag{21}$$

At this stage, the infinite-space Green's function in Fourier space for the isotropic point source $S(\boldsymbol{\rho}, \phi) = \delta(\boldsymbol{\rho})/(2\pi)$ is provided which is needed in the next section. To this end, we at first take the 2D Fourier transform $\psi_m(x, y) \longmapsto G_m(k_1, k_2)$ of system (10) which is given by

$$(ik_1 + k_2) G_{m-1}(\mathbf{k}) + (ik_1 - k_2) G_{m+1}(\mathbf{k}) + 2\sigma_m G_m(\mathbf{k}) = \frac{\delta_{m0}}{\pi}. \tag{22}$$

Similar as in the case of the homogenous solution a product ansatz can be used to obtain a simplified system which is only dependent on the length of the vector $\mathbf{k}$. An appropriate ansatz is $G_m(\mathbf{k}) = \chi_m(k) \exp(-im\phi_{\mathbf{k}})$ with $\tan\phi_{\mathbf{k}} = k_2/k_1$ so that the system of linear equations becomes

$$ik\chi_{m-1}(k) + ik\chi_{m+1}(k) + 2\sigma_m \chi_m(k) = \frac{\delta_{m0}}{\pi}. \tag{23}$$

Taking into account the normalized eigenvectors from the homogenous solution (16), we find the elements of Green's function in the 2D Fourier domain according to

$$G_m(\mathbf{k}) = \frac{e^{-im\phi_{\mathbf{k}}}}{\pi} \sum_{i=1}^{N} \frac{\varphi_0^{(i)} \varphi_m^{(i)}}{\lambda_i^2} \frac{1 + (-1)^m - i\sqrt{k_1^2 + k_2^2}\lambda_i [1 - (-1)^m]}{k_1^2 + k_2^2 + 1/\lambda_i^2}. \tag{24}$$

Next, we have to perform the 1D inverse Fourier transform $G_m(k_1, k_2) \longmapsto G_m(x, k)$ which can be carried out analytically. The result of the integration is

$$G_m(x, k) = \frac{1}{\pi} \sum_{i=1}^{N} \frac{\varphi_0^{(i)} \varphi_m^{(i)}}{\lambda_i^2} [\mathrm{sgn}(x)\sqrt{1 + (k\lambda_i)^2} - k\lambda_i]^m \frac{e^{-\sqrt{k^2 + 1/\lambda_i^2}|x|}}{\sqrt{k^2 + 1/\lambda_i^2}}, \tag{25}$$

where $\mathrm{sgn}(x)$ is the signum function. Therefore, the particular solution of the 2D RTE caused by a isotropic point source located at the origin of an infinite scattering medium becomes in Fourier space

$$I(x, k, \phi) = \sum_{m=-N}^{N} G_m(x, k) e^{im\phi}. \tag{26}$$

The Dirac delta line function

In this section, we describe the Dirac delta line function and integrate the obtained results in radiative transfer calculations. The 2D Dirac delta line function associated with the curve C can be defined as

$$\delta_C(\mathbf{x}) = \frac{1}{L}\int_C \delta(\mathbf{x} - \mathbf{x}(s))\mathrm{d}s, \tag{27}$$

where $\mathbf{x}(s)$ is an arbitrary contour in arc length parametrization and $L = \int_C \mathrm{d}s$ denotes the length of the curve. For the test function $f(\mathbf{x})$, we get

$$\int \delta_C(\mathbf{x}) f(\mathbf{x})\mathrm{d}\mathbf{x} = \frac{1}{L}\int_C f(\mathbf{x}(s))\mathrm{d}s. \tag{28}$$

In the limit $L \to 0$ we obtain the point source located at the starting point $\mathbf{x}_0$ according to

$$\lim_{L\to 0} \delta_C(\mathbf{x}) = \delta(\mathbf{x} - \mathbf{x}_0). \tag{29}$$

In particular when the line source is given explicitly by a function $y = f(x)$ defined in $x \in [x_1, x_2]$ Equation (27) can be alternatively written as

$$\delta_C(\mathbf{x}) = \frac{1}{L}\delta(y - f(x))\sqrt{1 + f'(x)^2}. \tag{30}$$

A similar expression can also be obtained for curves in polar form. The 2D Fourier transform of the delta line function is given by

$$\delta_C(\mathbf{k}) = \frac{1}{L}\int_C e^{-i\mathbf{k}\cdot\mathbf{x}(s)}\mathrm{d}s. \tag{31}$$

Let $g(\mathbf{x})$ be Green's function in two dimensions then the response $f(\mathbf{x})$ to an arbitrary curved line source becomes

$$f(\mathbf{x}) = \frac{1}{L}\int_C g(\mathbf{x} - \mathbf{x}(s))\mathrm{d}s. \tag{32}$$

In the following, we consider as an example an elliptic Dirac delta curve centered at the spatial point $(x_0, 0)$ with semi-major axis a and semi-minor axis b. The elliptic delta curve in parameter form is given by $\mathbf{x}(t) = (x_0 + a\cos t, b\sin t)$, where it is assumed that $x_0 \geq a$. The last restriction ensures that the elliptic curve is located completely in the half-plane $x \geq 0$. Figure 1 shows the elliptic line source located in the scattering half-plane for the values $x_0 = 2\,\mathrm{mm}$, $a = 1\,\mathrm{mm}$ and $b = 6\,\mathrm{mm}$.

For the further proceeding relation (32) is considered in the transformed space $(x, y) \longmapsto (x, k)$ which results in

$$f(x, k) = \frac{1}{L}\int_C g(x - x(s), k)e^{-iky(s)}\mathrm{d}s. \tag{33}$$

Here we intentionally take the test function $g(x, k) = e^{-\xi|x|}$ which is in view of the variable x strongly related to the derived elements (25) of Green's function. We evaluate the response along the boundary $x = 0$ so that the obtained result can be directly applied e.g. for evaluation of the reflectance caused by an elliptic line source.

The response at the boundary is given by

$$f(0, k) = \frac{e^{-\xi x_0}}{L}\int_0^{2\pi} e^{-\xi a\cos t}e^{-ikb\sin t}|\dot{\mathbf{x}}(t)|\mathrm{d}t, \tag{34}$$

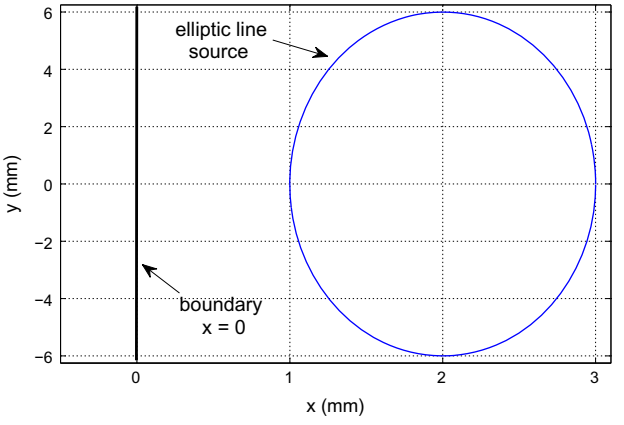

Figure 1. (Color online) Elliptic delta line source located in the scattering half-plane.

where $|\dot{\mathbf{x}}(t)| = \sqrt{a^2 \sin^2 t + b^2 \cos^2 t}$. In order to evaluate the above integral, we set

$$|\dot{\mathbf{x}}(t)| = \frac{1}{2\pi} \sum_{m=-\infty}^{\infty} A_m e^{-imt}, \tag{35}$$

where the coefficients are

$$A_m = \int_0^{2\pi} |\dot{\mathbf{x}}(t)| e^{imt} \mathrm{d}t. \tag{36}$$

Due to the given symmetry of the integrand the coefficients satisfy $A_{-m} = A_m$ and vanish when m is an odd number. The length L of the ellipse corresponds with the value A_0. For the further procedure we have to evaluate the following integral

$$\frac{1}{2\pi} \int_0^{2\pi} e^{-\xi a \cos t} e^{-ikb \sin t} e^{-imt} \mathrm{d}t = \frac{1}{\pi} \int_0^{\pi} e^{-\xi a \cos t} \cos(kb \sin t + mt) \mathrm{d}t. \tag{37}$$

By introducing 'formally' hyperbola coordinates according to

$$a\xi = R \cosh \varphi, \tag{38}$$

$$bk = R \sinh \varphi, \tag{39}$$

the integral can be written as

$$\frac{1}{2\pi} \int_0^{2\pi} e^{-R \cos(t - i\varphi)} e^{-imt} \mathrm{d}t, \tag{40}$$

for all $R, \varphi \in \mathbb{C}$ and evaluated analytically by taking into account the Laurent series

$$f(z) = e^{\frac{w}{2}(z+1/z)} = \sum_{m=-\infty}^{\infty} I_m(w) z^m, \tag{41}$$

where $w, z \in \mathbb{C}, |z| > 0$ and $I_m(w)$ is the modified Bessel function. The result of integration is

$$\frac{1}{2\pi}\int_0^{2\pi} e^{-R\cos(t-i\varphi)}e^{-imt}\mathrm{d}t = (-1)^m e^{m\varphi} I_m(R), \tag{42}$$

where $R = \sqrt{(a\xi)^2 - (bk)^2}$ and $\varphi = \ln[R/(a\xi - bk)]$. The response of the test function to the elliptic delta source evaluated at the boundary becomes in the 1D Fourier space

$$f(0,k) = e^{-\xi x_0} I_0(R) + e^{-\xi x_0}\frac{2}{A_0}\sum_{m=1}^{\infty} A_{2m}\cos(2m\varphi) I_{2m}(R). \tag{43}$$

In addition, by setting $\xi = -ik_1$, $k = k_2$, and $x_0 = 0$, we obtain directly the 2D Fourier transform of the elliptic line source centered at the origin according to

$$\delta_C(\mathbf{k}) = J_0(R) + \frac{2}{A_0}\sum_{m=1}^{\infty} A_{2m}\cos(2m\varphi) J_{2m}(R), \tag{44}$$

where $R = \sqrt{(ak_1)^2 + (bk_2)^2}$, $\tan\varphi = bk_2/(ak_1)$ and $J_m(x)$ is the Bessel function of the first kind. In the special case of a circle with radius ρ_0 Equations (43) and (44) simplify to $f(0,k) = e^{-\xi x_0} I_0(\rho_0\sqrt{\xi^2 - k^2})$ and $\delta_C(\mathbf{k}) = J_0(\rho_0|\mathbf{k}|)$, respectively. Note that the result for an ellipse which is centered at the point (x_0, y_0) with $y_0 \neq 0$ can be directly obtained by multiplying the right-hand side of Equation (43) with e^{-iky_0}.

Verification

In this section, the derived equations are verified and illustrated by comparisons with the Monte Carlo (MC) method. In the figures shown below the absorption coefficient and the reduced scattering coefficient of the semi-infinite medium are assumed to be $\mu_a = 0.01\,\mathrm{mm}^{-1}$ and $\mu_s' = (1-g)\mu_s = 1.0\,\mathrm{mm}^{-1}$, respectively. Furthermore, as an example we consider the Henyey–Greenstein (HG) scattering phase function for 2D media [23]

$$f(\hat{\mathbf{s}}\cdot\hat{\mathbf{s}}') = \frac{1}{2\pi}\frac{1-g^2}{1+g^2-2g(\hat{\mathbf{s}}\cdot\hat{\mathbf{s}}')} = \frac{1}{2\pi}\sum_{m=-\infty}^{\infty} g^{|m|}e^{im(\phi-\phi')}. \tag{45}$$

We start with the verification of the derived half-space Green's function of the 2D RTE by comparisons with the MC method. For the first comparison, we consider the case of perpendicular incident light beams assuming different spatial intensity distributions namely the Gaussian distribution (G), the uniform distribution (U) and the logistic distribution (L) which are given by

$$S_G(y) = \frac{1}{\sqrt{2\pi}\eta}e^{-\frac{y^2}{2\eta^2}}, \tag{46}$$

$$S_U(y) = \frac{1}{2\eta}\mathrm{rect}\frac{y}{2\eta}, \tag{47}$$

$$S_L(y) = \frac{1}{\eta}\frac{e^{-y/\eta}}{(1+e^{-y/\eta})^2}, \tag{48}$$

where $\mathrm{rect}(x) = \Theta(x+1/2) - \Theta(x-1/2)$ is the rectangular function and η denotes the radius of the beams. The corresponding characteristic functions in Fourier space are given by

$$S_G(k) = e^{-\eta^2 k^2/2}, \tag{49}$$

$$S_U(k) = \frac{\sin(\eta k)}{\eta k}, \tag{50}$$

$$S_L(k) = \frac{\pi \eta k}{\sinh(\pi \eta k)}. \tag{51}$$

Due to the convolution theorem we have to multiply the right-hand side of (17) with the above characteristic functions. Figure 2 displays the spatially-resolved reflectance caused by the above light beams. The derived solution (solid lines) coincidences with the reflectance obtained from the MC simulation (noisy curve).

For the next comparison, we consider an obliquely incident Gaussian beam with a radius $\eta_i = 0.1$ mm and the angle of incidence $\phi_i = 60°$ for both matched and mismatched BC. Note that in the case of refractive index mismatch at the boundary Snell's law leads to the angle of propagation $\phi_0 = \arcsin(1/n \sin \phi_i) \approx 38.21°$ and the beam radius projected onto the boundary becomes $\eta = \eta_i / \cos \phi_i = 0.2$ mm. In Figure 3, the solid lines correspond with the derived analytical solution whereas the noisy curves are the result obtained from the MC simulation. Both method are in agreement for matched and mismatched BC.

Next, we consider the case of an elliptic Dirac delta line source centered at the spatial point $(x_0, y_0) = (2\,\text{mm}, 0\,\text{mm})$ having a semi-major axis $a = 1$ mm in x-direction and different semi-minor axes b in y-direction, see for example Figure 1. Figure 4 shows the reflectance caused by the elliptic line source for both the derived analytical solution (solid lines) as well as for the MC simulation (noisy curves).

A sinusoidally Dirac delta line source given by the equation $x(y) = x_0 - a \sin(by)$ is considered in the strip $|y| \leq \pi/b$. Figure 5 shows for illustration the line source for the geometrical parameters $x_0 = 2$ mm, $a = 1.8$ mm and $b = 0.5$.

The resulting reflected light from the boundary is computed via the derived Green's function as well as the MC method and the results are depicted in Figure 6. For illustration, we additionally included the case $a = 0$ when the sinusoidally line source becomes the finite length straight line source $\delta_C(\mathbf{x}) = \delta(x - 2)\,\text{rect}[y/(4\pi)]/(4\pi)$. The analytical solution is given by the solid lines whereas the noisy curves are the result of the MC simulation.

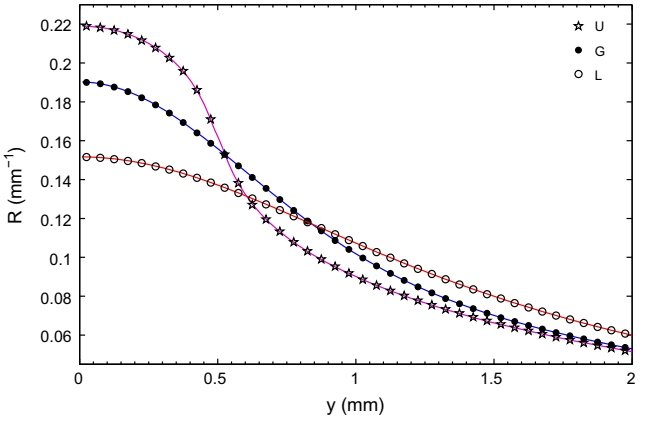

Figure 2. (Color online) Spatially-resolved reflectance as function of y for perpendicularly incident light beams with different spatial intensity distributions, where $\eta = 0.5$ mm. The anisotropy factor of the HG phase function is $g = 0.2$. The relative refractive index is $n = 1.4$.

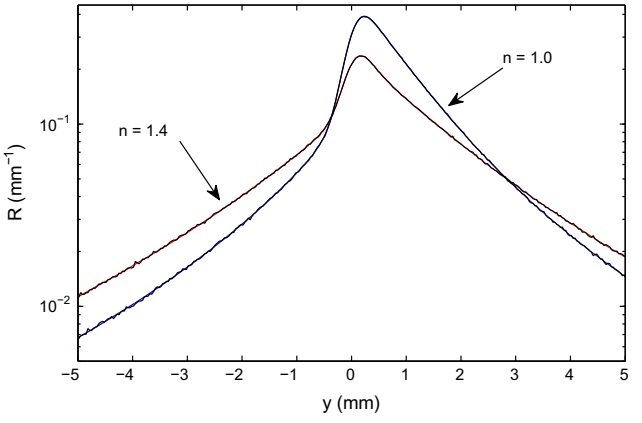

Figure 3. (Color online) Spatially-resolved reflectance as function of y for an obliquely incident Gaussian beam with radius $\eta_i = 0.1$ mm. The anisotropy factor of the HG phase function is $g = 0.8$.

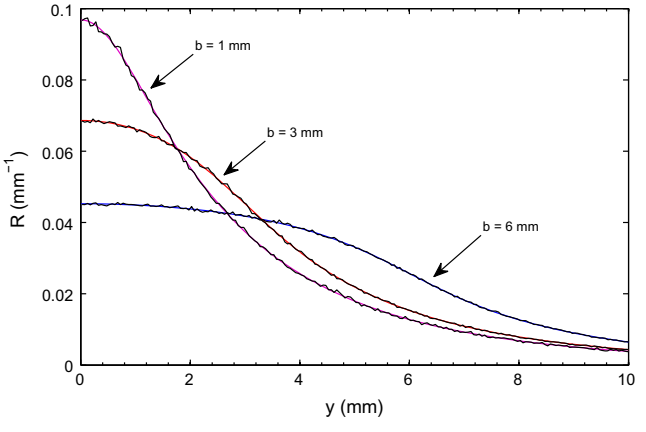

Figure 4. (Color online) Spatially-resolved reflectance as function of y due to different elliptic Dirac delta line sources. The anisotropy factor of the HG phase function is $g = 0.8$ and the relative refractive index is $n = 1.4$.

Finally, we consider the logarithmic spiral line source in the parameter form

$$x(t) = x_0 - ae^{bt} \sin t, \tag{52}$$

$$y(t) = y_0 + ae^{bt} \cos t, \tag{53}$$

where $0 \leq t < 2\pi$. Figure 7 shows the corresponding line source for the geometrical parameters $x_0 = 2$ mm, $a = 1$ mm, and $b = \ln(6)/(2\pi) \approx 0.2852$.

Figure 8 displays the resulting reflectance from the boundary of the half-plane caused by two different line sources. The figure contains both the analytical solution and the result of the MC simulation which is indicated by the circles.

We note that the transformation of the uniformly distributed random numbers $\Omega \in [0, 1)$ in the MC simulation leads in the case of the ellipse and the sinusoidally line source to an

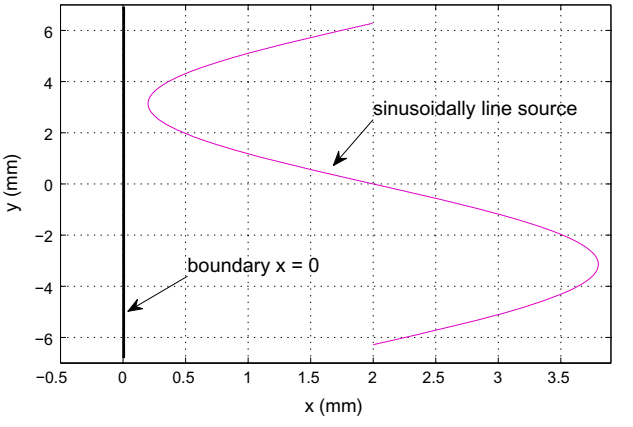

Figure 5. (Color online) Sinusoidally Dirac delta line source located in the scattering half-plane.

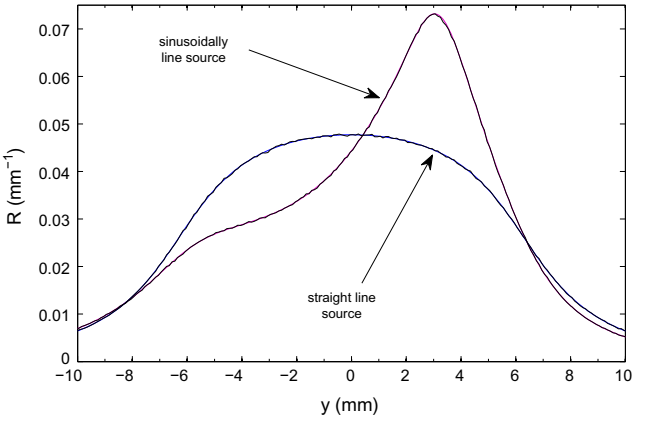

Figure 6. (Color online) Spatially-resolved reflectance as function of y for a sinusoidally Dirac delta line source. The anisotropy factor of the HG phase function and the relative refractive index are $g = 0.8$ and $n = 1.0$, respectively.

elliptic integral which must be inverted numerically. For the logarithmic spiral line source, this inversion can be carried out analytically so that the relation between the generated random number Ω and the curve parameter t is given by $t(\Omega) = \ln[1 + (e^{2\pi b} - 1)\Omega]/b$.

Discussion

In this article, the 2D RTE was solved for modeling the photon transport in the anisotropically scattering half-plane where the effect of Fresnel reflection at the boundary has also been taken into account. At the beginning, the half-space Green's function was derived in parts of the ballistic and diffuse contribution for the anisotropically scattering medium in the most probably maximal possible analytical form. Thus, it can be evaluated rapidly and accurately. Based on these results, we described analytically the photon propagation caused by arbitrary curved Dirac line sources where the elliptic curve was discussed in detail.

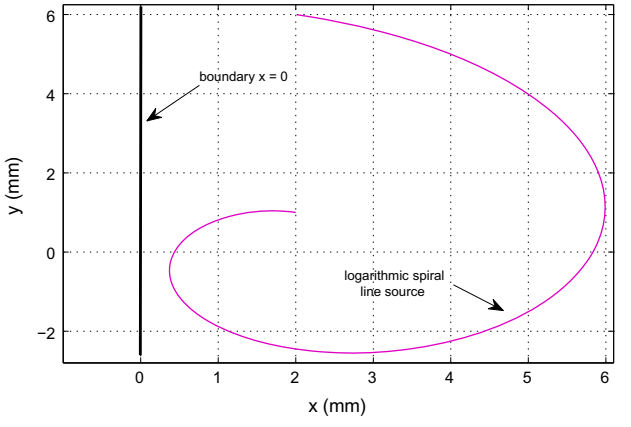

Figure 7. (Color online) Logarithmic spiral line source located in the scattering half-plane.

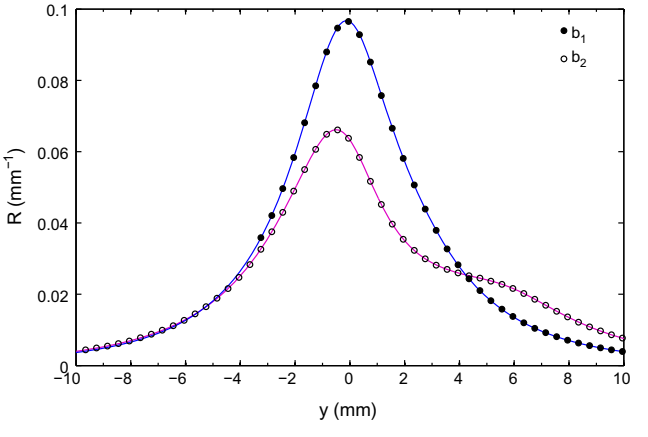

Figure 8. (Color online) Spatially-resolved reflectance as function of y for two different logarithmic spiral line sources. The geometrical parameters of the curves are $a = 1\,\text{mm}$, $b_1 = \ln(6)/(2\pi) \approx 0.2852$ and $b_2 = \ln(2)/(2\pi) \approx 0.1103$. The anisotropy factor of the HG phase function and the relative refractive index are $g = 0.8$ and $n = 1.0$, respectively.

The derived equations were successfully verified by comparisons with MC simulations showing, within the stochastic nature of the simulations, a good agreement. In the results section the Henyey–Greenstein function was applied as scattering phase function, but the derived equations can be used for an arbitrary rotationally invariant scattering phase function. We additionally note that although in this study we considered a curve embedded in a plane, the line source formalism can be directly extended to the 3D medium by changing the parametrization of the curve. The derived formulae can be applied for studying radiative transfer in anisotropically scattering half-planes, where external and internal sources can be considered. In addition, an important aspect is that it can be used for verification of results obtained by numerical methods for solving the RTE and/or to estimate the accuracy and the convergence of the applied approximation order.

References

[1] Chandrasekhar S. Radiative transfer. New York: Dover Publications; 1960.
[2] Case KM, Zweifel PF. Linear transport theory. New York: Addison-Wesley; 1967.
[3] Ishimaru A. Wave propagation and scattering in random media. New York: Academic Press; 1978.
[4] Martelli F, Del Bianco S, Ismaelli A, Zaccanti G. Light propagation through biological tissue and other diffusive media: theory, solutions, and software. Bellingham: SPIE Press; 2010.
[5] Markel VA. Modified spherical harmonics method for solving the radiative transport equation. Wave. Random Complex. 2004;14:L13–L19.
[6] Panasyuk G, Schotland JC, Markel VA. Radiative transport equation in rotated reference frames. J. Phys. A: Math. Gen. 2006;39:115–137.
[7] Williams MMR. The transport and diffusion theory of a line source in an infinite half-space with internal reflection. Ann. Nucl. Energ. 2007;34:910–921.
[8] Machida M, Panasyuk GY, Schotland JC, Markel VA. The Green's function for the radiative transport equation in the slab geometry. J. Phys. A: Math. Theor. 2010;43:065402.
[9] Liemert A, Kienle A. Light transport in three-dimensional semi-infinite scattering media. J. Opt. Soc. Am. A. 2012;29:1475–1481.
[10] Zhu L, Peskin CS. Simulation of a flapping flexible filament in a flowing soap film by the immersed boundary method. J. Comput. Phys. 2002;179:452–468.
[11] Nishimura N, Liu YJ. Thermal analysis of carbon-nanotube composites using a rigid-line inclusion model by the boundary integral equation method. Comput. Mech. 2004;35:1–10.
[12] Soedel W, Powder DP. A general Dirac delta function method for calculating the vibration response of plates to loads along arbitrarily curved lines. J. Sound Vib. 1976;65:29–35.
[13] Vynck K, Burresi M, Riboli F, Wiersma DS. Photon management in two-dimensional disordered media. Nat. Mat. 2012;11:1017–1022.
[14] Bal G, Freilikher V, Papanicolaou G, Ryzhik L. Wave transport along surfaces with random impedance. Phys. Rev. B. 2000;62:6228–6241.
[15] Meylan MH, Masson D. A linear Boltzmann equation to model wave scattering in the marginal ice zone. Ocean Model. 2006;11:417–427.
[16] Asadzadeh M, Larsen EW. Linear transport equations in flatland with small angular diffusion and their finite element approximations. Math. Comput. Model. 2008;47:495–514.
[17] Bögers C, MacLachlan S. An angular multigrid method for computing mono-energetic particle beams in Flatland. J. Comput. Phys. 2010;229:2914–2931.
[18] Johnson SR, Larsen EW. Diffusion boundary conditions in flatland geometry. Trans. Am. Nucl. Soc. 2011;105:446–448.
[19] Liemert A, Kienle A. Analytical approach for solving the radiative transfer equation in two-dimensional layered media. J. Quant. Spectrosc. Ra. 2012;113:559–564.
[20] Asllanaj F, Fumeron S. Modified finite volume method applied to radiative transfer in 2D complex geometries and graded index media. J. Quant. Spectrosc. Ra. 2010;111:274–279.
[21] Asllanaj F, Fumeron S. Applying a new computational method for biological tissue optics based on the time-dependent two-dimensional radiative transfer equation. J. Biomed. Opt. 2012;17:075007.
[22] Modest MF. Radiative heat transfer. London: Academic press; 2003.
[23] Heino J, Arridge SR, Sikora J, Somersalo E. Anisotropic effects in highly scattering media. Phys. Rev. E. 2003;68:031908.

Appendix: Transformation of Cartesian to elliptic coordinates

This appendix contains as an adjunct the formulae for transforming Cartesian into elliptic coordinates. The elliptic coordinate are related to the Cartesian by

$$x = f \cosh\xi \cos\eta \tag{54}$$

$$y = f \sinh\xi \sin\eta, \tag{55}$$

where $\xi \geq 0$, $\eta \in [0, 2\pi)$ and $f > 0$ is an arbitrary real number. For a given point (x, y), the corresponding coordinates (ξ, η) can be found by considering for $w = \xi + i\eta$ the real and imaginary parts of the function

$$f(w) = \cosh w = \cosh\xi \cos\eta + i \sinh\xi \sin\eta, \tag{56}$$

which are equal to $(x + iy)/f$. Therefore, the elliptic coordinates are obtained via inversion

$$\xi + i\eta = \operatorname{arcosh}\left(\frac{x + iy}{f}\right). \tag{57}$$

Setting $\alpha = (x^2 + y^2 + f^2)/(2f^2)$ and $\beta = x^2/f^2$ and taking the principal value of the inverse hyperbolic cosine leads to

$$\xi = \operatorname{arcosh}\sqrt{\alpha + \sqrt{\alpha^2 - \beta}}, \tag{58}$$

$$\eta = \begin{cases} \arccos[x/(f cosh\xi)] & y \geq 0 \\ -\arccos[x/(f cosh\xi)] & y < 0. \end{cases} \tag{59}$$

In addition, the Dirac delta line source in elliptic coordinates is given by

$$\delta_C(\xi, \eta) = \frac{1}{L} \frac{\delta(\xi - \xi_0)}{f\sqrt{\cosh^2\xi - \cos^2\eta}}, \tag{60}$$

where $\xi_0 = \operatorname{artanh}(b/a)$.